Contact Ion Pairs in the Bulk Affect Anion Interactions with Poly(*N*-Isopropylacrylamide)

Ellen E. Bruce,[†] Pho T. Bui,[‡] Mengrui Cao,[‡] Paul S. Cremer,[*,‡,¶] and Nico F. A. van der Vegt[*,†]

†*Eduard-Zintl-Institut für Anorganische und Physikalische Chemie, Technische Universität Darmstadt, D-64287 Darmstadt, Germany*

‡*Department of Chemistry, The Pennsylvania State University, University Park, PA 16802, USA*

¶*Department of Biochemistry and Molecular Biology, The Pennsylvania State University, University Park, PA 16802, USA*

E-mail: psc11@psu.edu; vandervegt@cpc.tu-darmstadt.de

Abstract

Salt effects on the solubility of uncharged polymers in aqueous solutions are usually dominated by the anions while the role of the cation with which they are paired is often ignored. In this study we examine the influence of three aqueous metal iodide salt solutions (LiI, NaI and CsI) on the phase transition temperature of poly(*N*-isopropylacrylamide) (PNIPAM) by measuring the turbidity change of the solutions. Weakly hydrated anions such as iodide are known to interact with the polymer and thereby lead to salting-in behavior at low salt concentration followed by salting-out behavior at higher salt concentration. When varying the cation type, an unexpected salting-out trend, $Cs^+ > Na^+ > Li^+$, is observed at higher salt concentrations. Using molecular dynamics simulations, it is demonstrated that this originates from contact ion pair formation in the bulk solution, which introduces a competition for iodide ions between the polymer and cations. The weakly hydrated cation Cs^+ forms contact ion pairs with I^- in the bulk solution, leading to depletion of CsI from the polymer–water interface. Microscopically this is correlated with the repulsion of iodide ions from the amide moiety.

Introduction

Since the end of the 19th century it has been known that the addition of salts to water affects properties of non-electrolytes dissolved in the solution.[1–3] Anions have, for example, the ability to precipitate macromolecules such as polymers and proteins from an aqueous solution. Their propensity to do so is ranked according to the Hofmeister series. The salting-out order of the anionic Hofmeister series is $CO_3^{2-} > SO_4^{2-} > S_2O_3^{2-} > H_2PO_4^- > F^- > Cl^- > Br^- > NO_3^- > I^- > ClO_4^- > SCN^-$. Anions are usually classified as weakly hydrated (right hand side of the series) or strongly hydrated (left hand side of the series). Weakly hydrated anions partition to nonpolar environments such as air–water[4] and polymer–water interfaces,[5,6] leading to a moderately increased polymer solubility (salting-in behavior). Strongly hydrated anions interact repulsively with and are depleted from the polymer surface instead (salting-out behavior).

Hofmeister effects have commonly been investigated with poly(*N*-isopropylacrylamide) (PNIPAM), a thermoresponsive water-soluble polymer broadly used as a model for polymers that exhibit a coil-to-globule transition at their lower critical solutions temperature (LCST). Many studies have focused on the effect of the anion in combination with sodium ions,[5,7–11] which are acting as charge balancing counterions. Indeed, Hofmeister phenomena are stronger for anions than for cations.[12] Despite the focus on anions, a typical consensus cationic Hofmeister series exists in the literature and the salting-out order for proteins is as follows:[13] $N(CH_3)_4^+ > NH_4^+ > Cs^+ > Rb^+ > K^+ > Na^+ > Li^+ > Ca^{2+} > Mg^{2+}$. This series is not as well understood as the anionic Hofmeister series. Interestingly, the order is opposite to the anionic series. That is, strongly hydrated cations (right hand side of the series) lead to salting-in and weakly hydrated cations (left hand side of the series) to salting-out behavior.

In this study, we report ion-specific effects on the LCST of PNIPAM in salt solutions consisting of the weakly hydrated iodide ion in combination with the alkali metal ions (Li^+, Na^+ and Cs^+). The addition of iodide induces salting-in behavior (swelling of the polymer chain) at low salt concentration due to direct ion binding.[5] This is followed by salting-out

behavior (collapse of the polymer chain) at higher concentration where solvation of the metal cations and anions in the bulk solution effectively causes the polymer to precipitate out.[5] We show that the LCST behavior (rate of change with salt concentration) of PNIPAM in metal iodide salt solutions depends on the specific nature of the cation. By employing all atom molecular dynamics (MD) simulations, this ion-specific behavior is elucidated at the molecular level.

Experimental methods

Materials. LiI (99.9% purity), NaI (99.5% purity) and CsI (99.9% purity) were all purchased from Sigma-Aldrich. PNIPAM, with a molecular weight of $186,800\,\mathrm{g/mol}$ and a polydispersity of 2.63, was purchased from Polymer Source, Inc.. A fixed amount of each salt was dissolved with PNIPAM in nitrogen-purged water (used to avoid iodine formation) to obtain solutions at each desired salt concentration ($25\,\mathrm{mM} - 1000\,\mathrm{mM}$).

Phase Transition Measurements. The change in turbidity was measured in solutions containing 10 mg/ml PNIPAM and various concentrations of LiI, NaI and CsI, respectively, to determine the LCST. An automated melting point apparatus (MPA 100 Optimal, Standford research Systems) with digital image processing software was used. A ramp rate of 1°C/min was used to measure the light scattering intensity as a function of temperature. More specifically, the LCST was determined from the onset of the light scattering increase relative to the flat and low intensity baseline observed at colder temperatures.[14] Details concerning the LCST measurements have been described before.[5]

Molecular Dynamics Simulations

System Setup and Simulations Details. All-atom simulations were carried out using the MD package Gromacs 2018.[15] The simulated systems were comprised of a PNIPAM 20-mer chain (isotactic-rich with 60% *meso* diad content) in aqueous salt solutions of LiI, NaI and CsI, respectively. The setup featured a stretched polymer chain extending through the periodic z-boundary. By connecting the head and tail, the chain had no end groups and can be considered as virtually infinite. This setup has been reported before.[16,17] By means of the GROMACS pull code a collapsed structure of the PNIPAM chain was pulled apart generating an elongated chain. The contour length of the 20-mer, $L_c = 5.32\,\mathrm{nm}$, together with the desired elongation of $\lambda = L_z/L_c = 0.88$ defined a box size in the z-direction to $L_z = 4.6839$ nm. The box dimensions in x- and y-direction were both initially 6.5 nm. The computational cost was minimized with this size, while interactions between periodic images were still prevented. A modified OPLS-AA force field[18] was used for the PNIPAM chain. LINCS[19] was utilized to constrain all bonds up to a fourth order expansion. The chain was solvated in water using the SPC/E[20] potential with the SETTLE[21] constraint algorithm keeping the internal geometry of the water molecule rigid. After energy minimization and equilibration, two water molecules at a time were replaced with an anion (I^-) and a cation (Li^+, Na^+ or Cs^+) until a salt concentration of 1 m (6216 water molecules, 112 cations and 112 anions) was achieved. While molality (moles/kg water) was used to describe the concentration in the simulations, molarity (moles/liter solution) was used in the experiments. The difference between the two units is negligible within the concentration range employed in this study. Nonpolarizable force fields were used for LiI, NaI[22] and CsI.[22] More specifically, the iodide ion model (4) and the cesium ion model (6) was used from the original reference.[22] See below for the details and validation of the LiI force field. Interactions between different atoms within the PNIPAM chain, as well as polymer–ion and polymer–water interactions were described with the geometric combination rule. The Lorentz–Berthelot combination rule was used to describe ion–ion and ion–water interactions. Furthermore, an additional

scaling factor of 0.9 was used for the dispersion interactions strength, ε_{ij}, between sodium ions (i) and iodide ions (j) according to the original force field.[22]

The systems were energy minimized followed by a 2 ns NVT equilibration run using a velocity-rescale thermostat.[23] Two consecutive NPT equilibration runs were subsequently performed. This started with a 2 ns equilibration using the Berendsen barostat[24] and the velocity-rescaling thermostat.[23] Next, a 3 ns equilibration was performed using the Parrinello-Rahman barostat[25,26] and the Nose–Hoover thermostat.[27,28] Finally, production runs of 100 ns were performed using the same barostat and thermostat as the last equilibration run. Coupling times of $\tau_{\mathrm{P}} = 2\,\mathrm{ps}$ and $\tau_{\mathrm{T}} = 1\,\mathrm{ps}$ were used for the barostats and thermostats, respectively, for all runs. All simulations were performed at 1 bar and 300 K. A semi-isotropic pressure coupling scheme in the x- and y-dimensions with the compressibilities $\kappa_{\mathrm{x,y}} = 4.5 \cdot 10^{-5}\,\mathrm{bar}^{-1}$, and $\kappa_{\mathrm{z}} = 0\,\mathrm{bar}^{-1}$ was applied in the z-dimension to maintain the stretched PNIPAM chain. Periodic boundary conditions were applied in all three directions. Furthermore, the particle mesh Ewald (PME) method[29] was used with a Fourier spacing of 0.12 nm, PME order 4, and a real space cutoff of 1.4 nm to treat the long-range electrostatic interactions. A cutoff radius of 1.4 nm was used for van der Waals interactions. No long-range pressure and energy corrections were applied. For the neighbor list, a cutoff distance of 1.4 nm was used and was updated every 0.002 ps. Configurations were saved every 1 ps and an integration time step of 2 fs was used as well.

Based on the general simulation details described above, four sets of simulations (I–Ⅳ) were conducted with the PNIPAM chain and one set without (V). Setup I corresponds to PNIPAM solvated in different salt solutions with all other parameters according to the description above. Setups Ⅱ and Ⅲ include modifications of the PNIPAM chain solvated in different salt solutions. Setup Ⅱ restrains PNIPAM. That is, a position restraint with a force constant of $1000\,\mathrm{kJmol^{-1}nm^{-2}}$ was applied to all atoms of the polymer chain in all three dimensions. Setup Ⅲ considers a "nonpolar" PNIPAM, i.e., a PNIPAM 20-mer with all partial atomic charges set equal to zero. Setup Ⅳ includes PNIPAM solvated in modi-

fied CsI solutions, i.e., using Lennard–Jones size parameters, $\sigma_{ij} = \lambda_\sigma(\sigma_i + \sigma_j)/2$, between cations ($i$) and anions ($j$) scaled with a factor λ_σ of 1.4 and 1.8, respectively. For setup V, bulk simulations of 1.0 m LiI, NaI and CsI were performed. A cubic box of the dimensions $4 \times 4 \times 4\,\mathrm{nm}^3$ with 2089 water molecules, 38 anions and 38 cations was used. Force fields and simulation parameters were the same as for the systems containing the polymer chain. Production runs were performed for 50 ns. If not stated otherwise, setup I was used.

Validation of Lithium Iodide Force Field. The LiI force field was comprised of a nonpolarizable Li^+ ion[30] combined with the iodide parameters taken from the NaI and CsI models.[22] This force field was validated against the osmotic coefficient and the procedure has been described before.[31,32] However, a flat bottom position restraint was used with a harmonic force to confine the ions. A cubic box, $5.4{\cdot}5.4{\cdot}5.4\,\mathrm{nm}^3$, filled with water, Li^+ and I^- ions was simulated using the GROMACS 2019 package.[15] Three different concentrations were examined: 0.2 m (water molecules= 5280, Li^+= 19 and I^-= 19), 0.6 m (water molecules= 5200, Li^+= 56 and I^-= 56) and 1.0 m (water molecules= 5130, Li^+= 93 and I^-=93). Energy minimization was performed, followed by a 0.25 ns NVT equilibration and a 1.5 ns NPT equilibration. Next, the simulation box was extended in the z-dimension to a total size of 10.8 nm, and the cubic box was placed in the middle. The new larger box was filled with water molecules leading to a total number of 10860, 10820 and 10810 water molecules for the three respective concentrations. Another energy minimization was carried out followed by a 0.25 ns NVT equilibration and a 1.5 ns NPT equilibration. Afterwards, production runs of 40 ns were performed. This was long enough to generate converged osmotic coefficients. The flat-bottom position restraints acted in the z-dimension. A semi-isotropic pressure couple scheme was therefore applied and only the x- and y-dimensions of the box were adjusted. Compressibilities of $\kappa_{\mathrm{x,y}} = 4.5 \cdot 10^{-5}\,\mathrm{bar}^{-1}$ and $\kappa_{\mathrm{z}} = 0\,\mathrm{bar}^{-1}$ were used. All other simulation settings were the same as for the simulations including the PNIPAM chain.

Anion–cation interactions were scaled to achieve agreement with the experimental os-

motic coefficients. This approach has been used before to effectively take polarization effects into account for nonpolarizable forcefields, and thereby avoid ion clustering.[22,33] A reasonable scaling of ε_{ij} between cations (i) and anions (j) did not affect the osmotic coefficients significantly. Instead, σ_{ij} interactions were scaled through $\sigma_{ij} = \lambda_\sigma(\sigma_i + \sigma_j)/2$, with a final scaling factor of $\lambda_\sigma = 0.93$. This scaling resulted in osmotic coefficients of $\phi = 0.96 \pm 0.12$ (0.966), $\phi = 1.01 \pm 0.11$ (1.022) and $\phi = 1.08 \pm 0.05$ (1.080) for the 0.2 m, 0.6 m and 1.0 m LiI solutions, respectively. The values in the parentheses are the corresponding experimentally[34] measured values.

Results

Phase Transition Temperatures and Ion Affinities. Figure 1 shows the phase transition temperature of PNIPAM as a function of metal iodide salt concentration. Non-linear behavior was seen in each case. The rate of change of the LCST with salt concentration was cation-specific. The decrease in the LCST at higher salt concentration was largest for CsI (orange squares) and smallest for LiI (blue triangles), while the turnover point took place at the highest salt concentration for LiI and the lowest for NaI (red circles).

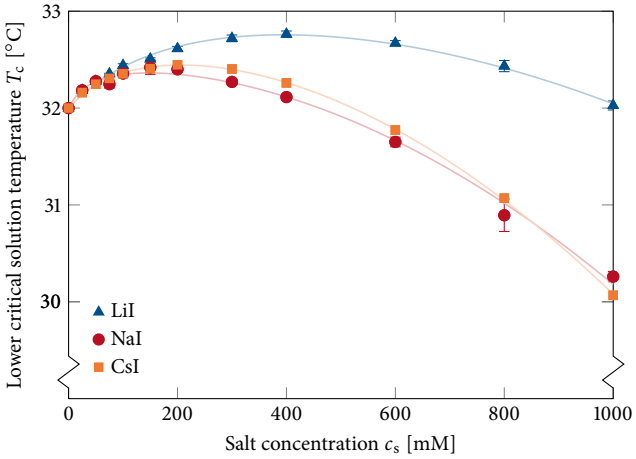

Figure 1. Lower critical solution temperature, T_c, of PNIPAM (10mg/ml) in LiI, NaI and CsI solutions, respectively, as a function of salt concentration, c_s. The symbols are data points representing an average of three measurements. The error bars were calculated as sample standard deviations, and are smaller than the size of the data points when not seen. The lines are guides to the eyes.

To understand the LCST trend, all-atom MD simulations were employed. Figure 2 shows the preferential binding coefficient[35] for indistinguishable ions (i.e., all cations and anions), Γ_{23}, for LiI (blue line), NaI (red line) and CsI (orange line) salt solutions (1 m) as a function of the closest distance to the polymer surface. The subscript 2 stands for the polymer and the subscript 3 for the ions, while the subscript 1 stands for water. Γ_{23} specifies the relation between the number of ions in the vicinity of the polymer and the statistical number in the bulk solution. A negative Γ_{23} value indicates ion depletion, while a positive Γ_{23} value indicates the favorable partitioning of ions to the polymer–water interface. LiI showed the least negative Γ_{23} value indicating the weakest depletion of ions, while CsI showed the most negative Γ_{23} and thereby the strongest depletion of the three salts considered. The slopes observed in the LCST curves at higher salt concentration (Figure 1) are proportional to the preferential binding coefficients (Figure 2) under the assumption that Γ_{23}, expressed per unit of solvent-accessible-surface area, does not depend on the conformation of the chain.[36] Thus, the simulation data for PNIPAM in LiI, NaI and CsI aqueous salt solutions are in qualitative agreement with the experiments.

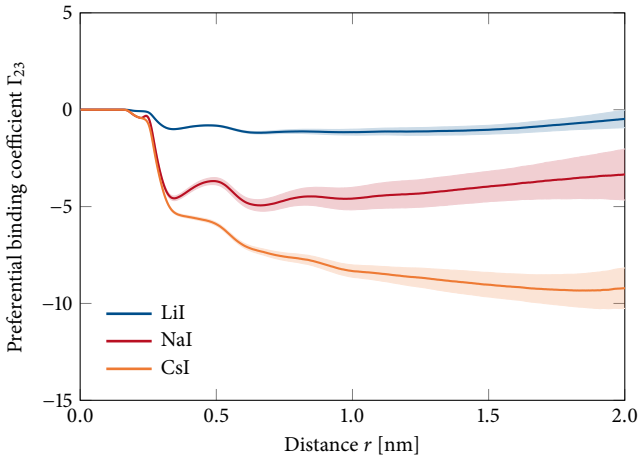

Figure 2. Preferential binding coefficient, Γ_{23}, to a PNIPAM 20-mer chain for LiI, NaI and CsI solutions, respectively, obtained from MD simulations. Γ_{23} is presented as a function of the proximal distance, r, i.e., the closest distance between an ion and an atom of the PNIPAM chain. In the calculation of Γ_{23}, cations and anions were treated as indistinguishable. The salt concentration was 1 m. The shaded intervals indicated the standard deviation of the mean, $\sigma/\sqrt{N}$, using sample standard deviation, σ, and $N = 10$ blocks.

Polymer–Ion Interactions. Interaction energies were calculated in order to eluci-

date the effect of cations on iodide's preferential interaction with PNIPAM, polymer–ion, polymer–water and monomer–solution (including all ions and water molecules) interactions. These are presented in Table 1. PNIPAM–anion interactions are more favorable than PNIPAM–cation interactions. This is reflected in the radial distribution functions (RDFs) between the polymer backbone and the anions, cations and all indistinguishable ions, respectively. The RDFs are shown in Figure 3 for all cases. The behavior of anions and cations can be seen both in the peak heights of the RDFs and in the cumulative number for the hydration shell of the 20-mer PNIPAM chain (distances up to $r = 0.922\,\mathrm{nm}$). The number of anions in the hydration shell of the 20-mer PNIPAM chain is 5.1, 4.8 and 3.9 for LiI, NaI and CsI, respectively. The number of cations is 4.5, 3.8 and 2.9, respectively. Furthermore, the PNIPAM–anion, PNIPAM–cation and PNIPAM–water interactions are cation-specific. PNIPAM–anion interactions follow the order LiI>NaI>CsI and the PNIPAM–cation follow the order LiI≈NaI>CsI. The PNIPAM–water interactions follow the order CsI>NaI≈LiI (Table 1). This agrees with the relative order between the above mentioned number of ions in the PNIPAM hydration shell for each salt type. That is, more favorable PNIPAM–ion interactions (at the cost of PNIPAM–water interactions) leads to more ions in the polymer hydration shell.

Spatial probability density maps were created to investigate the spatial position of the ions around the PNIPAM side chain. A distinct preferable position (yellow area) was seen for iodide ions close to the amide NH group and the terminal methyl groups (insets in Figure 3a). The spatial probability density of iodide ions was, however, affected by the type of cation. The probability at a certain threshold (see details in figure text) is significantly lower for CsI solution (orange box) than for LiI solution (blue box). A distinct preferable position (blue area) was also seen for lithium ions close to the amide oxygen (blue box in the inset of Figure 3b). This was not observed for cesium ions (orange box in the inset of Figure 3b) at the same threshold (see details in figure text), indicating weaker PNIPAM–Cs^+ interactions. Furthermore, the probability of finding iodide ions close to the polymer side chain was higher

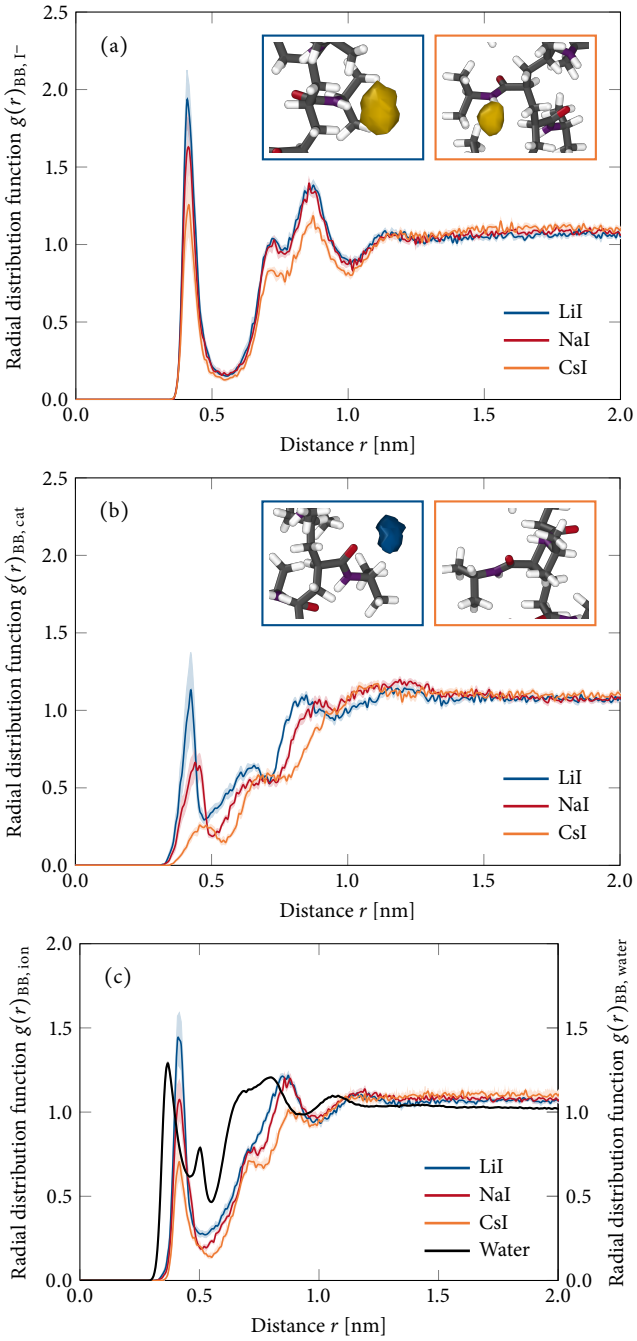

Figure 3. Normalized proximal radial distribution functions, $g(r)$, between the polymer backbone (BB) and (a) iodide (I^-), (b) the cations (cat) and (c) indistinguishable ions (ion) and water (right y-axis), respectively, as a function of the closest distance, r, from the polymer backbone for 1 m LiI, NaI and CsI solutions, respectively. The shaded intervals indicate the standard deviation of the mean, $\sigma/\sqrt{N}$, using sample standard deviation, σ, and $N = 10$ blocks, and are smaller than the line thickness representing the data when not seen. Insets in (a) show the spatial probability density maps of iodide ions (yellow) around the restrained PNIPAM chain (setup Ⅱ) in LiI (blue box) and CsI (orange box) solutions, respectively, using Ovito software.[37] The yellow area indicates five times the bulk anion number density and shows the amide NH group and the terminal methyl groups as the preferential interaction sites. Insets in (b) show the spatial probability density maps of lithium ions (blue) and cesium in LiI (blue box) and CsI (orange box) solutions (setup Ⅱ), respectively. The blue area indicates eight times the bulk cation number density and shows the amide oxygen as the preferential interaction site. Red represents oxygen atoms, purple nitrogen atoms, gray carbon atoms and white hydrogen atoms.

Table 1. Total interaction energies (sum of van der Waals and Coulombic interactions) between the 20-mer PNIPAM chain and the iodide, the three different cations and water molecules, respectively, for the three salt solutions (1 m). The energies were obtained by post processing the MD simulated trajectories using the rerun option in GROMACS, where the electrostatic energies were computed using a reaction field with a dielectric constant of 78. The average interaction energy of PNIPAM with one anion, one cation and one water molecule, respectively, are reported. Monomer–solution (including all ions and water molecules) energies represent the total interaction energy between one monomer and the solution (including all water molecules and ions). The given errors are the standard deviation of the mean, $\sigma/\sqrt{N}$, using sample standard deviation, σ, and $N = 10$ blocks.

Salt	PNIPAM–anion [kJ/mol]	PNIPAM–cation [kJ/mol]
LiI	-1.45 ± 0.07	-0.8 ± 0.2
NaI	-1.36 ± 0.08	-0.6 ± 0.2
CsI	-1.12 ± 0.08	-0.09 ± 0.07
Salt	PNIPAM–water [kJ/mol]	Monomer–solution [kJ/mol]
LiI	-0.417 ± 0.003	-142 ± 1
NaI	-0.418 ± 0.004	-141 ± 1
CsI	-0.429 ± 0.006	-140 ± 2

than for the respective cation. These results are in agreement with the observed weak, but favorable, interactions between the amide oxygen and cations, between the amide NH group and iodide ions and between the two terminal methyl groups and the iodide ions, respectively (not presented in Table 1). The interaction sites and the difference between strongly and weakly hydrated cations are in line with earlier studies of other (macro)molecules.[38–42] However, it has been experimentally shown that an NH moiety is not necessary for anion binding.[14]

The above mentioned interactions between part of the PNIPAM chain and ions include an electrostatic contribution. To obtain further insight into the role of these electrostatic interactions, MD simulations of a "nonpolar" PNIPAM molecule without partial atomic charges were performed in LiI, NaI, and CsI solutions (1 m), respectively. The absence of favorable ion–polymer electrostatic interactions correlates with vanishing ion specific binding to the polymer. This can be seen in Figure 4, where all three salts are depleted from the polymer surface to more or less the same extent (compare gray lines). When the partial

charges are reintroduced (blue, red and orange lines in Figure 4), the ion-specific salting-out series (CsI > NaI > LiI), observed in the experimental data (Figure 1), is recovered. Significantly, the LiI salt is less depleted when partial atomic charges on the polymer are reintroduced. This occurs due to favorable electrostatic interactions of iodide with the amide NH and lithium with the amide oxygen. The difference (PNIPAM chain vs. "nonpolar" PNIPAM chain) was larger for LiI than for NaI. This emerged from LiI interacting the strongest with the polymer chain, and thereby being affected the most in the absence of partial atomic charges. By contrast, CsI is instead more depleted when the partial atomic charges on the polymer are reintroduced. This is likely caused by favorable interactions of CsI ion pairs with the "nonpolar" PNIPAM surface. The "nonpolar" PNIPAM chains demonstrate that electrostatic interactions play a role in the ions' preferable affinity for the PNIPAM chain.

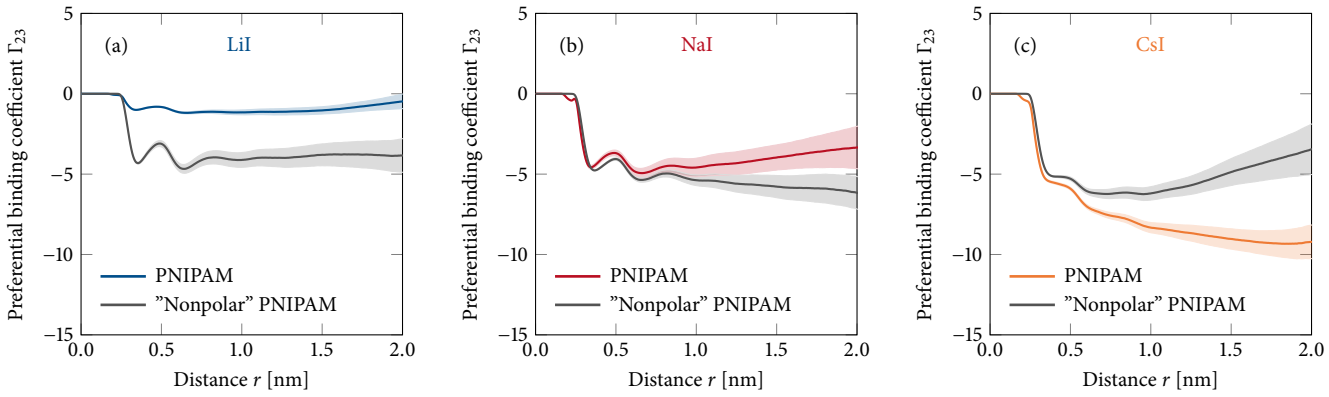

Figure 4. Preferential binding coefficients, Γ_{23}, to a PNIPAM 20-mer chain and a "nonpolar" PNIPAM 20-mer chain, respectively, for 1 m (a) LiI, (b) NaI and (c) CsI solutions (setup III) as a function of the proximal distance, r. The shaded intervals indicate the standard deviation of the mean, $\sigma/\sqrt{N}$, using sample standard deviation, σ, and $N = 10$ blocks. The preferential exclusion of ions from the "nonpolar" PNIPAM 20-mer chain is similar for the three salts in agreement with the air–water interface.

Thermodynamic Implications of Ion Pairing. Next, cation–anion pair formation in bulk solutions was investigated. Specifically, the fraction of contact ion-pairs (CIPs) in 1 m bulk solutions was investigated by integrating the cation–anion RDFs up to the first minimum. The fraction of CIPs was 0.82 for CsI, 0.11 for NaI and 0.07 for LiI. To investigate the influence of ion pairing in the bulk on the polymer–ion interactions, MD simulations

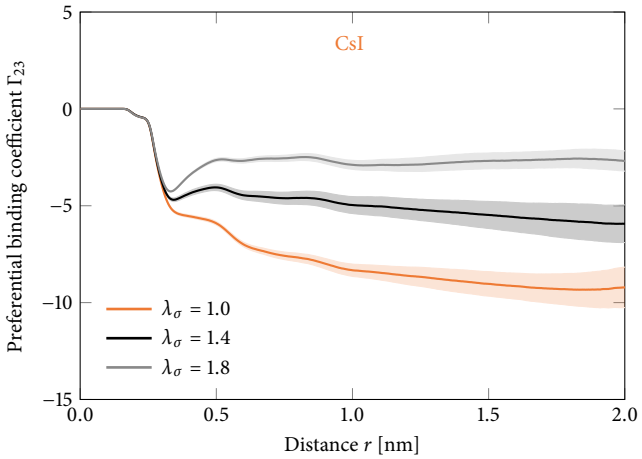

Figure 5. Preferential binding coefficients, Γ_{23}, to a PNIPAM 20-mer chain for 1 m CsI with different scaling factors, λ_σ, for their cation–anion Lennard–Jones size parameters (setup Ⅳ) as a function of the proximal distance, r. The shaded intervals indicate the standard deviation of the mean, $\sigma/\sqrt{N}$, using sample standard deviation, σ, and $N = 10$ blocks. Inhibiting CIP formation in bulk solution weakens CsI depletion from the polymer–water interface.

of PNIPAM chains in CsI solutions with modified ion-pairing ability (scaled cation–anion Lennard–Jones size parameter) were performed. A larger scaling factor, λ_σ, generated less ion pairing. Moreover, it led to less depletion from the PNIPAM chain. This can be seen by comparing the black and gray lines with the orange line in Figure 5.

To quantify the role of ion-pairs on a global level, Kirkwood–Buff integrals (KBIs) and non-ideality factors were calculated. The dependence of the LCST on the molar salt concentration (c_3) reflects how the chemical potential of the PNIPAM chain (2) depends on c_3. This dependency is provided by the Wyman–Tanford/Kirkwood–Buff relation:[35]

$$\left(\frac{\partial \mu_2}{\partial c_3}\right)_{p,T} = \frac{-RT\,\Gamma_{23}/c_3}{1 + c_3(G_{33} - G_{31})}, \tag{1}$$

where G_{33} and G_{31} denote the salt–salt and salt–water KBIs, respectively. This thermodynamic relation shows that the chemical potential of the polymer increases with salt when $\Gamma_{23} < 0$ (the denominator is alway positive), leading to a negative slope of the LCST (Figure 1) at high salt concentration. The role of ion pairing on a global level should be reflected by the term in the denominator of this equation, $G_{33} - G_{31}$, which accounts for the non-

ideality of the bulk electrolyte solution. This term is reported in Table 2, together with the non-ideality factor, $\frac{1}{1+c_3(G_{33}-G_{31})}$, and the preferential binding coefficients. Owing to ion pairing in bulk solution, $G_{33}-G_{31}$ is larger for CsI than for NaI (i.e., the non-ideality factor is lower and, especially, different from 1). The non-ideality factor therefore attenuates the difference between the values of the chemical potential derivatives $\left(\frac{\partial \mu_2}{\partial c_3}\right)_{p,T}$ of CsI and NaI obtained if only the values of Γ_{23} (Figure 2 and Table 2) of these two salts were considered and ideal solution behavior (i.e., equal salt-salt and salt-water affinities; $G_{33} = G_{31}$) would be assumed.

Table 2. Preferential binding coefficient, Γ_{23}, corresponding to a PNIPAM 20-mer with three different salts at 1 m (setup I), difference between salt–salt, G_{33}, and salt–water, G_{31}, Kirkwood–Buff integrals (KBIs) and non-ideality factor, $\frac{1}{1+c_3(G_{33}-G_{31})}$, for the three salt solutions at 1 m (setup V). Preferential binding coefficients and KBIs were calculated from converged running interval values between 1.5 nm and 2.0 nm. The KBIs were calculated with a RDF correction and Krüger volume correction,[43] see equation 8 in reference 44. The given errors are the standard deviation of the mean, $\sigma/\sqrt{N}$, using sample standard deviation, σ, and $N = 5$ blocks and propagation of uncertainty for the preferential binding coefficients. Errors for the difference in KBIs and non-ideality factor are calculated as sample standard deviation using propagation of uncertainty and are smaller than the reported accuracy.

Salt	Preferential binding coefficient Γ_{23}	Difference in KBIs $G_{33}-G_{31}$ [nm^3]	Non-ideality factor $\frac{1}{1+c_3(G_{33}-G_{31})}$
LiI	-0.8 ± 0.2	-0.130	1.14
NaI	-3.6 ± 0.5	-0.095	1.10
CsI	-9.2 ± 0.4	0.535	0.67

Discussion

Stronger salting-out behavior might be expected when I^- is combined with a high charge density cation (e.g., Li^+), and weaker salting-out behavior might be expected when combined with a low charge density cation (e.g., Cs^+). This expectation is based on the differences in cation hydration free energies[45] which indicate how easily a cation sheds its hydration shell when it approaches the polymer surface. Therefore, Li^+ would be expected to be more depleted than the weakly hydrated Cs^+, leading to a stronger salting-out behavior. Anions

have been shown to follow this behavior.[8,46–49] The LCST of PNIPAM in the presence of metal iodide salts shows instead the salting-out order: $Cs^+ > Na^+ > Li^+$ (Figure 1). This indicates that ion exclusion is subtle and charge density considerations alone cannot explain the Hofmeister effects for cations. The unexpected behavior of Li^+ in the view of its charge density has drawn attention before.[50–52]

The nonlinear LCST behavior with salt concentration (Figure 1) is indicative of polymer–ion interactions.[36] Another indication is that the observed difference in the LCST data for the different salts shows a discrepancy with ion partitioning to the air–water interface where Li^+, Na^+ and Cs^+ are all excluded to about the same extent.[53] While electrostatic polymer–ion interactions are crucial for the binding of ions to specific sites on the PNIPAM surface and lead to ion specific features in the preferential binding coefficients (Figure 4), the partitioning of ions in the hydration shell of the "nonpolar" PNIPAM chain instead resembles the behavior at the air–water interface. This is in line with earlier studies showing that polar groups draw cations, that are usually excluded from an air–water interface,[54] into the interfacial region.[55]

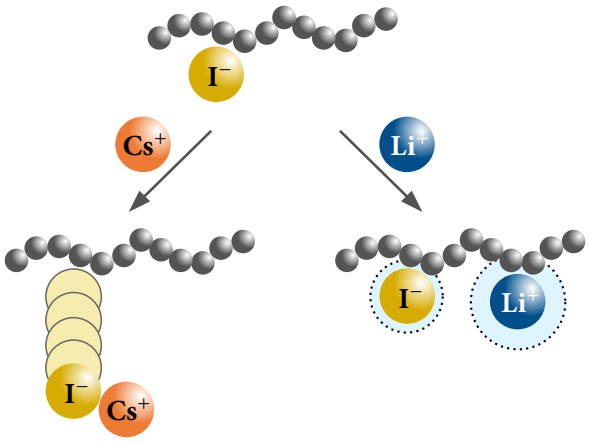

Figure 6. Schematic illustration of the mechanisms of the cation-specific effect on PNIPAM–iodide interactions. The chain of gray spheres represents the polymer. The black dotted circles represent the hydration shells. It should be noted that the relative size of the polymer and ions are not drawn to scale.

PNIPAM–iodide interactions are stronger than PNIPAM–cation interactions, but the cation type has an impact on all polymer–ion interactions and thereby on the dependence of the LCST on salt concentration (Figure 3 and Table 1). The underlying mechanisms of

cation-specific effects on the PNIPAM–iodide interactions proposed in this study are depicted in Figure 6. Various experiments and MD analyses show that aqueous salt solutions do not form statistical mixtures (equally distributed ions), but rather show ion pairing and ion clustering.[56] The more weakly hydrated the cation is, the larger is the propensity for the weakly hydrated iodide to form CIPs with it. This is in line with the law of matching water affinities.[57] In an aqueous CsI solution, CIPs are formed due to both ions being weakly hydrated. This leads to charge neutrality for some ion-pairs and a loss of the possibility for iodide ions to electrostatically interact with the amide NH group on the polymer (left side of Figure 6). The ions are thereby repelled from the polymer–water interface, and the LCST is strongly suppressed (salting-out of PNIPAM). The degree to which ion pairing is decisive for the partitioning of ions to the polymer–water interface was demonstrated in this study (Figure 5). When Cs^+ and I^- are prevented from forming electrically neutral CIPs in the simulations, weaker salt depletion occurs. In an aqueous LiI solution, hardly any CIPs are formed. Instead, the iodide ions can independently move to the polymer–water interface and interact electrostatically with the amide NH group (right side of Figure 6). Lithium ions follow to avoid charge separation. Lithium ions also show weakly favorable interactions with the polymer chain themselves (Table 1), namely with the amide oxygen.

Concurrent interactions of iodide (Figure 3a) and lithium ions (Figure 3b) with PNIPAM leads to a smaller suppression of the LCST in LiI solution than in CsI solution. However, both the relative differences in the preferential binding coefficients (Figure 2) and the large differences in the number of CIPs observed in bulk solution are not reflected in the LCST curves (Figure 1), in particularly not for NaI and CsI. This is due to a compensation of two effects. While ion pairing drives iodide away from the polymer and causes a decrease of Γ_{23}, it further causes a decrease in the effective concentration (activity) of the salt as expressed by the larger value of the denominator in equation 1 for CsI than for NaI (Figure 2 and Table 2). Ion pairing in bulk solution should therefore have two thermodynamic implications: i) it leads to a weaker iodide interaction with the polymer, contributing to salting out; ii)

the corresponding, weaker salt–water interaction attenuates the role of solvent-excluded volume[58] (an effective force related to the entropy of the solvent that drives polymer compaction and hydrophobic interaction), contributing to salting in. The observed LCST behavior with increasing concentration of iodide salts (Figure 1) is thus determined by the balance of these two effects.

Salting-in behavior is observed at low salt concentration for all salts due to the free energy favorable partitioning of weakly hydrated iodide ions to the polymer surface. At higher salt concentrations, the probability for ion pairing in the bulk is higher. This leads to a competition between PNIPAM–iodide interactions and iodide–cation interactions in the bulk. The latter dominates for weakly hydrated cations (e.g., Cs^+) since they readily form CIPs and they do not show preferable interaction with the polymer. This explains why the driving force to compact the polymer chain (salting-out behavior) sets in at a lower concentration for CsI than for LiI.

The nonadditive and dependent behavior for how ions affect polymer solubility explained in this study updates earlier ideas[53,59] about simple additive and independent ion specific interactions. In addition to polymer–ion interactions, ion–counterion interactions are demonstrated to be crucial for Hofmeister effects and follows up earlier ideas about that ion–ion interactions, and not only individual ion interactions, are of importance for the understanding of ion-specific effects.[60] However, the effect of ion pairs on the LCST of polymers will probably depend on the type of ion pair, and the identity of the cations and anions involved. The effects in this work apply to salts containing a weakly hydrated anion. For salts containing a more strongly hydrated anion, such as chloride, occurrence of solvent-shared ion pairs together with weak, but favorable, polymer–cation interactions instead cause a mitigation of chloride's salting-out effect when paired with a strongly hydrated cation.[61]

Conclusions

We have shown that the LCST behavior of PNIPAM in iodide salt solutions is affected by the specific combination of the anion and the cation. Electrostatic interactions of anions and cations with the amide group play a role in ion interactions with PNIPAM and the type of cation affects the PNIPAM–iodide interaction. A weakly hydrated cation (e.g., Cs^+) results in weaker iodide affinity, while a strongly hydrated cation (e.g., Li^+) results in stronger iodide affinity. This speaks against simple additivity and provides yet another example where observed changes in polymer solubility are due to nonadditive effects. The polymer–iodide interaction is inversely correlated with anion–cation ion pairing in the bulk. As we move from the strongly hydrated cation Li^+ to the weakly hydrated cation Cs^+, the affinity for CIP formation with iodide ions in the bulk increases. Such charge neutralization leads to a larger loss in the electrostatic interactions with the polymer chain, explaining the greater decrease in the LCST for iodide salts containing Cs^+ compared to Li^+.

Acknowledgement

The authors thank the LOEWE project iNAPO funded by the Ministry of Higher Education, Research and the Arts (HMWK) of the state of Hessen. PSC thanks the National Science Foundation (CHE-1709735) for funding. Additionally, the authors thank Luis Vollmer for the help with the validation of the LiI force field.

References

(1) Hofmeister, F. Zur Lehre yon der Wirkung der Salze. *Naunyn-Schmiedeberg's Arch. Pharmacol* **1888**, *24*, 247–260.

(2) Hofmeister, F. Zur Lehre von der Wirkung der Salze. *Naunyn-Schmiedeberg's Arch. Pharmacol* **1888**, *25*, 1–30.

(3) Kunz, W.; Henle, J.; Ninham, B. W. 'Zur Lehre von der Wirkung der Salze' (About the Science of the Effect of Salts): Franz Hofmeister's Historical Papers. *Curr. Opin. Colloid Interface Sci.* **2004**, *9*, 19–37.

(4) Jungwirth, P.; Tobias, D. J. Molecular Structure of Salt Solutions: A New View of the Interface with Implications for Heterogeneous Atmospheric Chemistry. *J. Phys. Chem. B* **2001**, *105*, 10468–10472.

(5) Zhang, Y.; Furyk, S.; Bergbreiter, D. E.; Cremer, P. S. Specific Ion Effects on the Water Solubility of Macromolecules: PNIPAM and the Hofmeister Series. *J. Am. Chem. Soc.* **2005**, *127*, 14505–14510.

(6) Cho, Y.; Zhang, Y.; Christensen, T.; Sagle, L. B.; Chilkoti, A.; Cremer, P. S. Effects of Hofmeister Anions on the Phase Transition Temperature of Elastin-Like Polypeptides. *J. Phys. Chem. B* **2008**, *112*, 13765–13771.

(7) Furyk, S.; Zhang, Y.; Ortiz-Acosta, D.; Cremer, P. S.; Bergbreiter, D. E. Effects of End Group Polarity and Molecular Weight on the Lower Critical Solution Temperature of Poly(*N*-Isopropylacrylamide). *J. Polym. Sci. Part A Polym. Chem.* **2006**, *44*, 1492–1501.

(8) Zhang, Y.; Cremer, P. S. Interactions Between Macromolecules and Ions: The Hofmeister Series. *Curr. Opin. Chem. Biol.* **2006**, *10*, 658–663.

(9) Zhang, Y.; Furyk, S.; Sagle, L. B.; Cho, Y.; Bergbreiter, D. E.; Cremer, P. S. Effects of Hofmeister Anions on the LCST of PNIPAM as a Function of Molecular Weight. *J. Phys. Chem. C* **2007**, *111*, 8916–8924.

(10) Zhang, Y.; Cremer, P. S. Chemistry of Hofmeister Anions and Osmolytes. *Annu. Rev. Phys. Chem.* **2010**, *61*, 63–83.

(11) Pérez-Fuentes, L.; Bastos-González, D.; Faraudo, J.; Drummond, C. On the Salting out of Benzene by Alkali Chlorideseffect of Organic and Inorganic Ions on the Lower Critical Solution Transition and Aggregation of PNIPAM. *Soft Matter* **2018**, *14*, 7818–7828.

(12) Gibb, B. C. Hofmeister's Curse. *Nat. Chem.* **2019**, *11*, 963–965.

(13) Traube, J. The Attraction Pressure. *J. Phys. Chem.* **1910**, *14*, 452–470.

(14) Rembert, K. B.; Okur, H. I.; Hilty, C.; Cremer, P. S. An NH Moiety is Not Required for Anion Binding to Amides in Aqueous Solution. *Langmuir* **2015**, *31*, 3459–3464.

(15) Abraham, M. J.; Murtola, T.; Schulz, R.; Páll, S.; Smith, J. C.; Hess, B.; Lindah, E. GROMACS: High Performance Molecular Simulations Through Multi-Level Parallelism from Laptops to Supercomputers. *SoftwareX* **2015**, *1-2*, 19–25.

(16) Horinek, D.; Netz, R. R. Can Simulations Quantitatively Predict Peptide Transfer Free Energies to Urea Solutions? Thermodynamic Concepts and Force Field Limitations. *J. Phys. Chem. A* **2011**, *115*, 6125–6136.

(17) Kanduč, M.; Chudoba, R.; Palczynski, K.; Kim, W. K.; Roa, R.; Dzubiella, J. Selective Solute Adsorption and Partitioning Around Single Pnipam Chains. *Phys. Chem. Chem. Phys.* **2017**, *19*, 5906–5916.

(18) Dalgicdir, C.; van der Vegt, N. F. A. Improved Temperature Behavior of PNIPAM in Water with a Modified OPLS Model. *J. Phys. Chem. B* **2019**, *123*, 3875–3883.

(19) Hess, B.; Bekker, H.; Berendsen, H. J. C.; Fraaije, J. G. E. M. LINCS: A Linear Constraint Solver for Molecular Simulations. *J. Comput. Chem.* **1997**, *18*, 1463–1472.

(20) Berendsen, H. J. C.; Grigera, J. R.; Straatsma, T. P. The Missing Term in Effective Pair Potentials. *J. Phys. Chem.* **1987**, *91*, 6269–6271.

(21) Miyamoto, S.; Kollman, P. A. Settle: An Analytical Version of the Shake and Rattle Algorithm for Rigid Water Models. *J. Comput. Chem.* **1992**, *13*, 952–962.

(22) Fyta, M.; Netz, R. R. Ionic Force Field Optimization Based on Single-Ion and Ion-Pair Solvation Properties: Going Beyond Standard Mixing Rules. *J. Chem. Phys.* **2012**, *136*, 124103.

(23) Bussi, G.; Donadio, D.; Parrinello, M. Canonical Sampling Through Velocity Rescaling. *J. Chem. Phys.* **2007**, *126*, 014101.

(24) Berendsen, H. J. C.; Postma, J. P. M.; van Gunsteren, W. F.; DiNola, A.; Haak, J. R. Molecular Dynamics with Coupling to an External Bath. *J. Chem. Phys.* **1984**, *81*, 3684–3690.

(25) Parrinello, M.; Rahman, A. Polymorphic Transitions in Single Crystals: A New Molecular Dynamics Method. *J. Appl. Phys.* **1981**, *52*, 7182–7190.

(26) Nosé, S.; Klein, M. L. Constant Pressure Molecular Dynamics for Molecular Systems. *Mol. Phys.* **1983**, *50*, 1055–1076.

(27) Nosé, S. A Molecular Dynamics Method for Simulations in the Canonical Ensemble. *Mol. Phys.* **1984**, *52*, 255–268.

(28) Hoover, W. G. Canonical Dynamics: Equilibrium Phase-Space Distributions. *Phys. Rev. A* **1985**, *31*, 1695–1697.

(29) Darden, T.; York, D.; Pedersen, L. Particle Mesh Ewald: An $N\cdot\mathrm{Log}(N)$ Method for Ewald Sums in Large Systems. *J. Chem. Phys.* **1993**, *98*, 10089–10092.

(30) Hess, B.; van der Vegt, N. F. A. Cation Specific Binding with Protein Surface Charges. *Proc. Natl. Acad. Sci. U. S. A.* **2009**, *106*, 13296–13300.

(31) Luo, Y.; Roux, B. Simulation of Osmotic Pressure in Concentrated Aqueous Salt Solutions. *J. Phys. Chem. Lett.* **2010**, *1*, 183–189.

(32) Bruce, E. E.; van der Vegt, N. F. A. Does an Electronic Continuum Correction Improve Effective Short-Range Ion-Ion Interactions in Aqueous Solution? *J. Chem. Phys.* **2018**, *148*, 222816.

(33) Bruce, E. E.; Bui, P. T.; Rogers, B. A.; Cremer, P. S.; van der Vegt, N. F. A. Non-Additive Ion Effects Drive Both Collapse and Swelling of Thermoresponsive Polymers in Water. *J. Am. Chem. Soc.* **2019**, *141*, 6609–6616.

(34) Robinson, R. A.; Stokes, R. H. *Electrolyte Solutions*, 2nd ed.; Butterworth & Co. Ltd.: London, 2002.

(35) Pierce, V.; Kang, M.; Aburi, M.; Weerasinghe, S.; Smith, P. E. Recent Applications of Kirkwood–Buff Theory to Biological Systems. *Cell Biochem. Biophys.* **2008**, *50*, 1–22.

(36) Heyda, J.; Dzubiella, J. Thermodynamic Description of Hofmeister Effects on the LCST of Thermosensitive Polymers. *J. Phys. Chem. B* **2014**, *118*, 10979–10988.

(37) Stukowski, A. Visualization and Analysis of Atomistic Simulation Data with Ovito–the Open Visualization Tool. *Model. Simul. Mater. Sci. Eng.* **2010**, *18*, 015012.

(38) Vrbka, L.; Vondrášek, J.; Jagoda-Cwiklik, B.; Vácha, R.; Jungwirth, P. Quantification and Rationalization of the Higher Affinity of Sodium Over Potassium to Protein Surfaces. *Proc. Natl. Acad. Sci. U. S. A.* **2006**, *103*, 15440–15444.

(39) Heyda, J.; Vincent, J. C.; Tobias, D. J.; Dzubiella, J.; Jungwirth, P. Ion Specificity at the Peptide Bond: Molecular Dynamics Simulations of N-Methylacetamide in Aqueous Salt Solutions. *J. Phys. Chem. B* **2010**, *114*, 1213–1220.

(40) Kherb, J.; Flores, S. C.; Cremer, P. S. Role of Carboxylate Side Chains in the Cation Hofmeister Series. *J. Phys. Chem. B* **2012**, *116*, 7389–7397.

(41) Okur, H. I.; Kherb, J.; Cremer, P. S. Cations Bind Only Weakly to Amides in Aqueous Solutions. *J. Am. Chem. Soc.* **2013**, *135*, 5062–5067.

(42) Okur, H. I.; Hladílková, J.; Rembert, K. B.; Cho, Y.; Heyda, J.; Dzubiella, J.; Cremer, P. S.; Jungwirth, P. Beyond the Hofmeister Series: Ion-Specific Effects on Proteins and Their Biological Functions. *J. Phys. Chem. B* **2017**, *121*, 1997–2014.

(43) Krüger, P.; Schnell, S. K.; Bedeaux, D.; Kjelstrup, S.; Vlugt, T. J. H.; Simon, J.-M. Kirkwood–Buff Integrals for Finite Volumes. *J. Phys. Chem. Lett.* **2013**, *4*, 235–238.

(44) Milzetti, J.; Nayar, D.; van der Vegt, N. F. A. Convergence of Kirkwood–Buff Integrals of Ideal and Nonideal Aqueous Solutions Using Molecular Dynamics Simulations. *J. Phys. Chem. B* **2018**, *122*, 5515–5526.

(45) Marcus, Y. *Ion Properties*; Marcel Dekker, Inc.: New York, 1997; pp 120–121.

(46) Baldwin, R. L. How Hofmeister Ion Interactions Affect Protein Stability. *Biophys. J.* **1996**, *71*, 2056–2063.

(47) Melander, W.; Horváth, C. Salt Effects on Hydrophobic Interactions in Precipitation and Chromatography of Proteins: An Interpretation of the Lyotropic Series. *Arch. Biochem. Biophys.* **1977**, *183*, 200–215.

(48) Arakawa, T.; Timasheff, S. N. Preferential Interactions of Proteins with Salts in Concentrated Solutions. *Biochemistry* **1982**, *21*, 6545–6552.

(49) Arakawa, T.; Timasheff, S. N. Mechanism of Protein Salting in and Salting Out by Divalent Cation Salts: Balance between Hydration and Salt Binding. *Biochemistry* **1984**, *23*, 5912–5923.

(50) Thomas, A. S.; Elcock, A. H. Molecular Dynamics Simulations of Hydrophobic Associations in Aqueous Salt Solutions Indicate a Connection between Water Hydrogen Bonding and the Hofmeister Effect. *J. Am. Chem. Soc.* **2007**, *129*, 14887–14898.

(51) Thomas, A. S.; Elcock, A. H. Molecular Dynamics Simulations Predict a Favorable and

Unique Mode of Interaction between Lithium (Li+) Ions and Hydrophobic Molecules in Aqueous Solution. *J. Chem. Theory Comput.* **2011**, *7*, 818–824.

(52) Ganguly, P.; Hajari, T.; van der Vegt, N. F. A. Molecular Simulation Study on Hofmeister Cations and the Aqueous Solubility of Benzene. *J. Phys. Chem. B* **2014**, *118*, 5331–5339.

(53) Pegram, L. M.; Record Jr., M. T. Hofmeister Salt Effects on Surface Tension Arise from Partitioning of Anions and Cations between Bulk Water and the Air–Water Interface. *J. Phys. Chem. B* **2007**, *111*, 5411–5417.

(54) Jungwirth, P.; Tobias, D. J. Specific Ion Effects at the Air/Water Interface. *Chem. Rev.* **2006**, *106*, 1259–1281.

(55) Krisch, M. J.; D'Auria, R.; Brown, M. A.; Tobias, D. J.; Hemminger, C.; Ammann, M.; Starr, D. E.; Bluhm, H. The Effect of an Organic Surfactant on the Liquid–Vapor Interface of an Electrolyte Solution. *J. Phys. Chem. C* **2007**, *111*, 13497–13509.

(56) van der Vegt, N. F. A.; Haldrup, K.; Roke, S.; Zheng, J.; Lund, M.; Bakker, H. J. Water-Mediated Ion Pairing: Occurrence and Relevance. *Chem. Rev.* **2016**, *116*, 7626–7641.

(57) Collins, K. D. Charge Density-Dependent Strength of Hydration and Biological Structure. *Biophys. J.* **1997**, *72*, 65–76.

(58) Bruce, E. E.; van der Vegt, N. F. A. Molecular scale solvation in complex solutions. *J. Am. Chem. Soc.* **2019**, *141*, 12948–12956.

(59) Pegram, L. M.; Record Jr., M. T. Thermodynamic Origin of Hofmeister Ion Effects. *J. Phys. Chem. B* **2008**, *112*, 9428–9436.

(60) Jungwirth, P.; Cremer, P. S. Beyond Hofmeister. *Nat. Chem.* **2014**, *6*, 261–263.

(61) Bruce, E. E.; Okur, H. I.; Stegmaier, S.; Drexler, C. I.; Rogers, B. A.; van der Vegt, N. F. A.; Roke, S.; Cremer, P. S. Molecular Mechanism for the Interactions of Hofmeister Cations with Macromolecules in Aqueous Solution. *J. Am. Chem. Soc.* **2020**, https://dx.doi.org/10.1021/jacs.0c07214.

Graphical TOC Entry